Central European Journal of Energetic Materials
ISSN 1733-7178; e-ISSN 2353-1843

Cent. Eur. J. Energ. Mater. 2018, *15*(4): 610-628; DOI 10.22211/cejem/100683

Research paper

High Penetration Performance of Powder Metallurgy Copper-Tungsten Shaped Charge Liners

Tamer Elshenawy[1], Gamal Abdo[2], Ahmed Elbeih[3O*]

1) Technical Research Center, Cairo, Egypt
2) Mechanical Engineering Department, Modern Academy for Engineering and Technology, Cairo, Egypt
3) Military Technical College, Kobry Elkobbah, 11765, Cairo, Egypt
O - https://orcid.org/0000-0001-9143-0804
[*]E-mail: elbeih.czech@gmail.com

Abstract: Copper tungsten liner manufactured using uniaxial pressing technique has been characterized numerically and experimentally in comparison with a baseline shaped charge copper liner produced by deep drawing technique. The jet properties resulted from these two shaped charges were different according to their liner types and relevant densities which affect the resultant penetration depths into rolled homogeneous armour (RHA) targets. Different copper-tungsten powder liners have been studied and analysed using Autodyn hydrocode, from which an optimum powder design was chosen based on its maximum jet kinetic energy that can be coherent. The compacted liner elastic properties have been measured using SONELASTIC apparatus, whereas its real density is determined using helium gas pycnometer. Baseline copper liner obtained by deep drawing technique of uniform density exhibited lower penetration depth in comparison with the copper-tungsten liner (higher density powder). Besides, the penetration crater resulted from the powder liner showed clean hole without clogging because there was no massive slug as in the case of the copper liners. Experimental field tests of the two liners against (RHA) targets exhibited different penetrations depths, which have been accounted in this research.

Keywords: penetration, copper-tungsten liner, RDX, jet formation, Autodyn

1 Introduction

Various liner materials have been used to manufacture shaped charge liners using different techniques [1]. Zirconium, copper, silver, steel, titanium depleted uranium liners were studied according to their jet break-up time [2-4] and effective jet length [2]. Glass liner was tested and exhibited a large breakup time in comparison with the traditional copper liner at large stand-off distances [5]. Compacted powder pressing materials acted as a shaped charge liners were patented in 2001 by Reese *et al.* [6] as a shaped charge oil well perforator liner for oil and gas well field completion. Stinson *et al.* have patented the methodology for producing single phase tungsten or molybdenum liners for warhead application using hot isostatic pressing technique, after which the final liner dimensions were obtained by machining [7]. Walters *et al.* have tested un-sintered copper tungsten liners against steel targets at short stand-off distances using OMNI shaped charge and described the bulk spreading jet particles using flash x-ray radiograph [8]. Halliburton energy service, USA, has also patented some different powder liners including tungsten, copper, lead, tantalum and molybdenum with their different loading densities to test them in the oil industry. Their invention has been implemented in the oil industry as oil well perforator to complete the well [9]. Hirsch and Mayseless discussed and analysed the characteristics of the shaped charge powder jet and its penetration capability into soft and hard targets [10]. Zhang *et al.* have measured the jet velocity of copper-tungsten powder liner and the effect of both water and air as a medium on the attenuation of its jet tip velocity [11]. Glenn used composite liner composed of copper, tungsten, graphite and tin powders for oil well perforating concrete targets [12]. All the discussed liners produce different profiles of jet and slug based on the liner design and the type of the liner material as well as the required purpose. For instance, the un-sintered powder mixture liners were introduced to resolve the problem caused by the massive copper slug that clogs the oil well after it has been completed. They require certain chemical treatment and further additional cost to remove the massive slug and re-open the penetrated hole again.

Our research is devoted to design precursor shaped charge of a thermobaric warhead capable of achieving large perforation depth into armour body without clogging the penetrated hole. The thermobaric main warhead has its designated crew causalities even with a very small thermobaric charge. After the main armour has been perforated by shaped charge jet, a prolonged reflected shock waves generated from thermobaric weapon has a lethal mechanism and crew causalities. In addition, the behind armour effect would be expected to enhance within the confined limited space of the tank [13].

In this paper, alternative liner material design is introduced depending on the powder technology, in which the produced jet can create a clean hole into armour material without clogging the perforated hole. The powder liner is designed based on extensive comparative study of its mechanical properties and its density effect on the produced jet characteristics and its coherency criteria. The expected jet characteristics of both the optimized powder design and the baseline copper liner are obtained using Autodyn hydrocode. Two different techniques were used in this research for the manufacture of shaped charge liners; one of them is used for production of copper-tungsten powder (as a green products un-sintered liner), while the other is deep drawing technique for production of copper liner. The density of the prepared green product liners obtained from the uniaxial powder pressing technique has been measured using helium gas pycnometer. On the other hand, the elastic properties of the compacted powder liner have been obtained using SONELASTIC advanced Impulse excitation technique apparatus. Extensive numerical trials using Autodyn hydrocode have been performed to study the effect of liner properties on the coherency of the produced jet and its characteristics. Selected copper-tungsten liner has been produced and studied experimentally in comparison with copper liner as a baseline. The performance of both the compacted copper-tungsten powder and the deep drawn copper liners have been assessed by the static firing of the two shaped charges including these two liners against RHA steel targets.

2 Experimental work

2.1 Manufacturing of liner by different methods

Copper-Tungsten liners (CTL) have been manufactured using uni-axial pressing technique. The base diameter of the liners was 30 mm, a cone apex angle 44° and the liner wall thickness was 1.2 mm. All the powders were obtained from Sigma Aldrich UK, limited. The optimum mixture of the powder liner composition was copper 35%, tungsten 55%, tin (coating mixture) 8.5% and graphite (as a lubricant) 1.5% mass percentages. The average grain size of copper, tungsten, tin and graphite was 3 μm, 0.6 μm, 45 μm, 20 μm, respectively. The drying temperature of the powder was 60 °C, after which the powders were mixed together with the specified ratio for 30 min. until the mixture became homogeneous. The pressing process of the mixture was performed uniformly at low rate of 2 MPa per second up to maximum value of 350 MPa using Instron uni-axial hydraulic press. The product is called “green product” which is a brittle material without sintering. Schematic drawing of the uniaxial

powder pressing die, punch and ejector and their necessary accessories are shown in Figure 1.

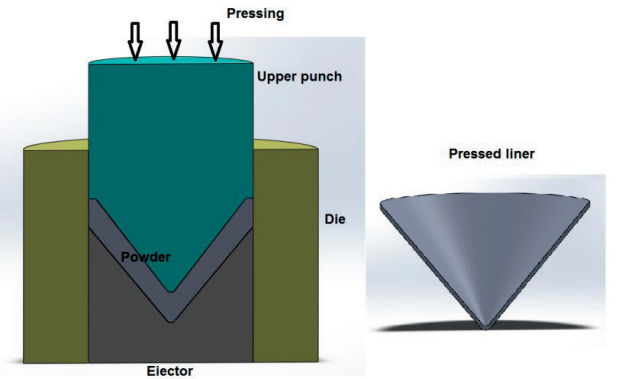

Figure 1. Uni-axial pressing sketch

The baseline copper liner used in this research was electrolytic Copper of grade C10100 OFHC (Oxygen Free High Conductivity Copper). This material has high purity (99.99%), very low oxygen and phosphorus contents for relatively high ductility (which is needed for the jet material to sustain longer breakup time and have a better coherent performance) [14]. The copper liner was manufactured using the deep drawing technique, because this technique is economical and efficient for producing large quantities of small calibre liners with a reasonable accuracy [15]. It starts by cutting a circular copper disc and applying five steps of drawing by hydraulic press with an intermediate annealing of 400 °C (2 min) to decrease the strain hardening and maintain the material ductility [15]. Photo for the two tested liners is shown in Figure 2.

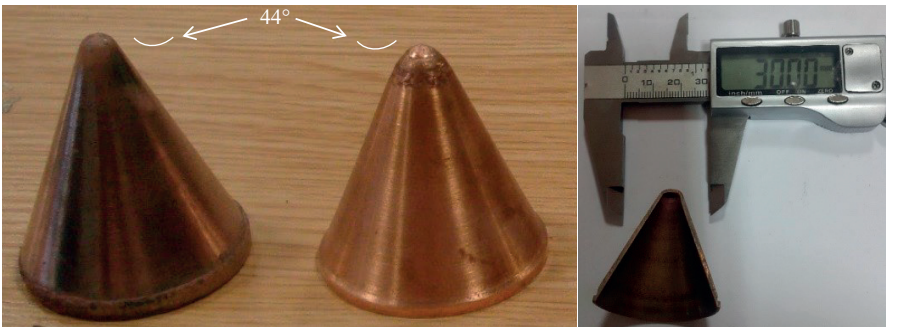

Figure 2. Photo of the two tested liners; copper–tungsten liner powder (left) and the baseline copper (right)

2.2 Preparation of explosive filler

Plastic bonded explosive (PBX) based on 1,3,5-trinitro-1,3,5-triazacyclohexane (RDX) bonded by polyurethane matrix was prepared for filling of the shaped charges [16]. RDX is a product of Eurenco Co., Paris, France. The polyurethane polymeric matrix contains hydroxyl-terminated polybutadiene (HTPB, product of ARCO Co.), hexamethylenediisocyanate (HMDI, product of Shandong Yucheng Yiao Technology Co.Ltd., China), tris-1-(2-methylaziridinyl)phosphine oxide (MAPO, product of Hangzhou Yuhao Chemical Technology Co. Ltd., China) and dioctyladipate (DOA, product of Island Pyrochemical Industries, China). The production method was based on placing the liquid ingredients, HTPB (prepolymer), MAPO (bonding agent) and DOA (plasticizer) in a vertical mixer and mixed for 20 min at 40 °C followed by vacuum mixing for a further 20 min to drive out entrapped air. Then RDX was added in three portions during 30 min. Finally, HMDI (curing agent) was added to the mixture at 55 °C and the ingredients were mixed for a further 30 min under vacuum. The prepared PBX cured at 60 ±2 °C for seven days under vacuum. The cured HTPB binder system was prepared with an NCO/OH ratio of 1.3. MAPO was 0.5 wt.%, while DOA was 20 wt.% of the total mass of the binder system. The prepared PBX contained 88 wt.% of RDX and 12 wt.% of polyurethane, and was designated as RDX-HTPB.

2.3 Sensitivity and detonation properties of PBX

Impact sensitivity of the prepared PBX was measured by using impact tester with exchangeable anvil (Julius Peters) [17] and the friction sensitivity was determined by using a BAM friction test apparatus [17]. Using the Probit analysis technique [18], the 50% probability of initiation is reported in Table 1 as impact and friction sensitivities. The initiation reactivity and the shock sensitivity of RDX-HTPB were recorded in Ref. [19, 20]. The detonation velocity was measured by using EXPLOMET-FO-2000 produced by KONTINITRO AG [21]. Three samples in the form of cylinders with diameter 21 mm and length of 300 mm were tested and the average value is reported in Table 1 as detonation velocity. The detonation properties were calculated by using EXPLO5 thermodynamic code [22]. BKWN set of parameters for the BKW EOS was applied (a = 0.5, b = 0.298, k = 10.50, Q = 6620). The calculated detonation properties (detonation velocity, D, heat of detonation, Q_d, and detonation pressure, P) are reported in Table 1.

2.4 Shaped charges static penetration test

The outer casing of the tested shaped charges were steel 4340 with an average wall thickness 2 mm manufactured by using CNC from cylinder of diameter

40 mm. The prepared PBX (RDX-HTPB) was used for filling the shaped charges, where 30 g was weighted and casted under vacuum into the steel container before the curing process, followed by pressing the liner slowly to avoid cracking and failure of the green product powder liner. The prepared shaped charges left for 7 days at 60 °C to complete the curing process of the PBX. The two charges are placed and fixed over the RHA steel layers with 40 mm stand-off distance as shown in Figure 3. Laminated layers of RHA steel armour with total thickness of 150 mm are used in the penetration test. Detonator no. 8 was used for electrically firing the shaped charges. The depth of penetration was measured for both charges as a measure of the performance of both compacted powder and baseline copper sheet liners. Besides, the crater profile and remaining slug closing the crater hole is also considered as the main objective of this research.

Figure 3. Test setup and the manufactured shaped charges

Table 1. The detonation characteristics of the used explosive load

Sample	Experimental data				EXPLO 5 code		
	Impact energy [J]	Friction force [N]	Loading density [g/cm^3]	Detonation velocity, D [m/s]	Detonation velocity calc., D_{cal} [m/s]	Detonation pressure, P [GPa]	Heat of detonation, Q_d [kJ/kg]
RDX-HTPB	11.8	360	1.62	7982	7836	24.01	5681

2.5 Mechanical testing of the compacted liner mechanical properties

The compacted powder mechanical properties have been determined for different liner compositions using SONELASTIC advanced Impulse excitation technique apparatus released by ATCP Physical Engineering, Brazil. Sonelastic® Software consists of a transient vibrations analyser, from which the frequencies are extracted to calculate the elastic moduli and respective decay rate for the damping ratio calculation. The software identifies the vibration frequencies and respective damping ratios by processing the sample's acoustic response to a mechanical impulse (light impact on the sample). This technique is described in the ASTM E1876 and correlated standards. The SONELASTIC enabled us to estimate E; Young's modulus, K; bulk modulus, ν; the Poisson's ratio and bulk density of the tested compacted liner specimen.

3 Numerical calculations

3. 1 Autodyn Numerical hydrocode

Three different Autodyn numerical schemes have been implemented in the current research; these schemes are the jetting analysis, jet formation and jet interaction (penetration) with the RHA target. The jetting analysis based on the unsteady state PER theory [23] is used to calculate the jet and the slug velocities and masses as well as the resultant kinetic energy and momentum of the jet. The collapse, flow and jet velocities, the liner collapse and deflection angles as well as the jet kinetic energy of the jet are all estimated as an attached HTML file when the jetting analysis is finished. The jet formation is performed using Euler solver based on continuum mechanics to obtain the jet profiles at different time stages. The output of this scheme will be a jet having certain momentum at certain time as is used as the input of Lagrange-Lagrange jet-target interaction scheme. The last scheme is the penetration of the jet with the RHA target, which is modeled using Lagrange method. In this scheme, the jet obtained from the second scheme is remapped to Lagrangian moving grids and impacts the RHA target. The overall crater profile inside the RHA target is monitored. Interested reader for further details such as erosion strain effect and mesh sensitivity analysis as well as validity and verification of this hydrocode refer to Ref. [24].

3.2 Material model

The equation of state (EOS) for the used high explosive is Jones-Wilkins-Lee (JWL) equation. The values of the experimental constants for some

explosives have been determined from sideways plate push dynamic test experiments [25] and the cylinder expansion test [26-28]. The explosive loading density was 1.62 g/cm^3, parameter A in the JWL EOS is 8.1658×10^8 kPa and parameter B is 1.6228×10^7 kPa. R_1 and R_2 equal to 4.067 and 1.377, respectively, while constant $\omega = 0.185$. The detonation velocity =7836 m/s, while the detonation pressure $=2.40\times10^7$ kPa and the C-J Energy *per* unit volume $= 9.204\times10^6$ kJ/m^3.

The copper liner material has density of 8.9 g/cm^3 and is modeled by linear EOS of bulk modulus 1.0×10^8 kPa and reference temperature 293 K, while its strength model is neglected for extremely large pressure on the liner walls according to jetting tutorial by Autodyn century dynamics [29]. The copper-tungsten powder liner is modeled using the real densities obtained by pycnometer, whereas the bulk modulus is obtained using the SONELASTIC apparatus for each liner element individually.

The material used for the charge case was steel 4340 of density 7.83 g/cm^3 with the shock EOS of parameter C_1 = 4569 m/s and S_1 = 1.4. Johnson Cook strength model was used with the steel casing of shear modulus 8.18×10^7 kPa, yield strength of 3.5×10^5 kPa and reference strain rate is 1.

The RHA target material has a density of 7.86 and shock EOS of Gruneisen coefficient 1.67 and parameter C_1 = 4610 m/s and S_1 = 1.73. The strength model used with the RHA target is the Von Mises criteria of shear modulus 6.41×10^7 kPa, and yield stress of 1.5×10^6 kPa.

4 Results

4.1 Optimum liner selection

The elastic properties of the compacted copper-tungsten powders obtained using the SONELASTIC apparatus are listed in Table 2. The difference in the elastic properties may be attributed to the difference in the mixture bulk density of its ingredients because both the two effective materials; copper and tungsten have different grain sizes. Thus the overall bulk density may vary and so the young's modulus as well as Poisson's ratio have different values for the five compacted powder compositions. According to Table 2, as the tungsten percent increases in the powder mixture, the expected average bulk grain size decreases, thus the young's modulus decreases; whereas the Poison's ratio increases. This result is similar to that obtained for nanocrystalline tungsten [30].

The elastic properties are needed to quantify the sound speed limit that must not be exceeded when compared to the maximum flow velocity of the liner element during its collapse. Cowan and Holtzman [31] presented an overview

for the jetting condition criteria in the explosive welding applications. Chou *et al.* [32] summarized the jetting and coherence conditions, which determines the maximum coherent flow velocity in the subsonic regime; *i.e.* ($V_2 \leq C_L$), where V_2 is the maximum flow velocity of the liner element during its collapse and C_L is the longitudinal sound speed of the solid liner material given by

$$C_L = \sqrt{3\frac{1-\nu}{1+\nu}}C_o \tag{1}$$

in which, $C_o = \sqrt{K/\rho_o}$

where ρ_o is the jet density, K is the bulk modulus and ν is the Poisson's ratio.

The conditions of the jet formation and its cohesion was confirmed by Harrison [33] and Walker [34] experimentally where flash X-ray was used to show that a coherent jet is formed when $V_2 < C_L$. Therefore, coherency criterion for a given shaped charge, is necessary during the selection of its optimum liner material.

The coherency criteria for the studied five compacted liners is applied for the flow velocity estimated from the shaped charge jetting analysis model obtained from Autodyn. The sound speed limit is compared to the maximum flow velocity obtained from AUTODYN for each liner. Table 3 lists the various speed limits and the maximum flow velocity indicating the coherency jet state. W30-Cu60 liner type exhibited non coherent jet because its flow velocity exceeds that of the sound speed limit. The other four liners have coherent jet, in which is liner ingredient may be recommended. Other factors should be considered such as powder availability and its cost. Our final decision was to select the W35-Cu55 design, which achieved 0.987 of its maximum flow velocity that can be obtained with coherent jet according to Table 3. Besides, this powder contains the lowest possible percent of tungsten that can produce coherent jet, which has the lowest price because the tungsten powder price is five times that of the used copper powder.

Table 2. The elastic properties obtained from the SONELASTIC apparatus for copper-tungsten powders

Code	Density [g/cm^3]	E [GPa]	ν	K [GPa]
W30-Cu60	10.325	50	0.36	59.52
W35-Cu55	10.775	49	0.38	68.06
W40-Cu50	11.225	47	0.39	71.21
W45-Cu45	11.675	45	0.40	75.00
W60-Cu30	13.025	42	0.41	77.78

Table 3. The elastic properties and relevant jet coherency calculations of compacted powder mixtures

Code	C_o [m/s]	C_L [m/s]	C_L/C_o	Max. flow velocity [m/s]	V_2/C_L	Coherent
W30-Cu60	2401.05	2852.87	1.190	2926	1.026	No
W35-Cu55	2513.18	2917.70	1.161	2880	0.987	Yes
W40-Cu50	2518.74	2890.03	1.147	2843	0.984	Yes
W45-Cu45	2534.56	2873.92	1.134	2800	0.974	Yes
W60-Cu30	2443.65	2737.89	1.120	2682	0.980	Yes

Powder mixtures have different densities based on their initial powder composition design, which in turn yield different collapse velocities and therefore result in different jet tip velocities due to explosive-metal Gurney configurations and unsteady state PER theory [35]. The real density distribution was considered in the jets formed from powdered metal liners and its effect on the penetration has also been discussed analytically [36-38] and experimentally [39]. The jetting summary for the studied four liner compositions is listed in Table 4 with the jet summaries. Composition W35-Cu55 shows the largest coherent jet kinetic energy of 41.8 kJ, which is also predicted to have the largest penetration depth when compared to other studied liners. Figure 4 shows the jet velocity-cumulative jet mass for the studied five powder liners. As the liner density decreases, it collapse velocity and flow velocity increase, thus its jet tip velocity increases, whereas its jet percent from the total liner mass decreases. The five curves have similar profile but little difference showing the density effect on the jet velocity and its cumulative mass cannot be neglected. Unfortunately, the liner of the highest velocity, which is W30-Cu60, has non-coherent jet, therefore next W35-Cu55 liner is confirmed to be the optimum one.

Table 4. Theoretical jetting calculations of the different initial powder compositions

Code	Liner mass [g]	Jet mass [g]	Jet [%]	Jet K.E. [kJ]	Jet tip velocity [m/s]	Max. flow velocity [m/s]	Is jet coherent?
W30-Cu60	31.6	5.4	17.1	41.8	6274	2926	No
W35-Cu55	33.0	5.6	17.0	41.4	6176	2880	Yes
W40-Cu50	34.4	5.8	16.8	41.1	6088	2843	Yes
W45-Cu45	35.7	5.9	16.6	40.8	5994	2800	Yes
W60-Cu30	39.9	6.4	16.1	39.7	5732	2682	Yes

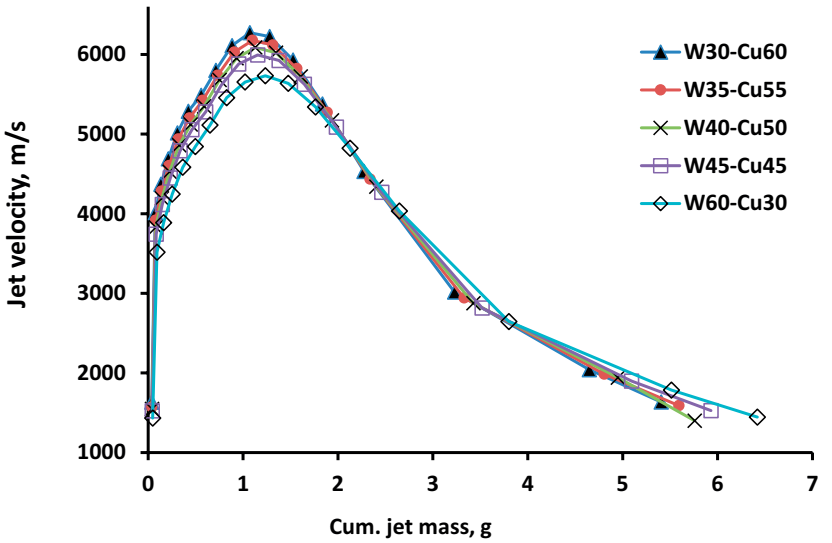

Figure 4. The jet velocity-cumulative jet mass for the studied five powder liners

4.2 Real liner characterization

Since the density of the produced green product liner is crucial during the estimation of shaped charge jetting analysis, it has to be measured precisely to guarantee the correctness and the reliability of the used hydrocode. The AccuPyc1330 helium gas pycnometer has been used for determine liner density by measuring the occupied volume according to the pressure change of helium in a calibrated volume. The weighed sample at an accuracy of 0.1 mg is determined at different heights from the liner base. Every compacted powder liner is divided into tiny pieces and marked according to the liner height positions, after which the helium gas pycnometer is used to determine its density as shown in Figure 5. The relation between density of the liner and the distance from the apex is represented on Figure 5 for the practical measurements of the tested pressed powder liner. The non-uniform density of uniaxial pressed liner is obtained due to the pressing forces distribution along the liner cone part and the non- regular stresses distribution along the inclined liner conical side. The obtained density profile is used within the Autodyn hydrocode in order to estimate the jet profile and its penetration capability into steel RHA targets.

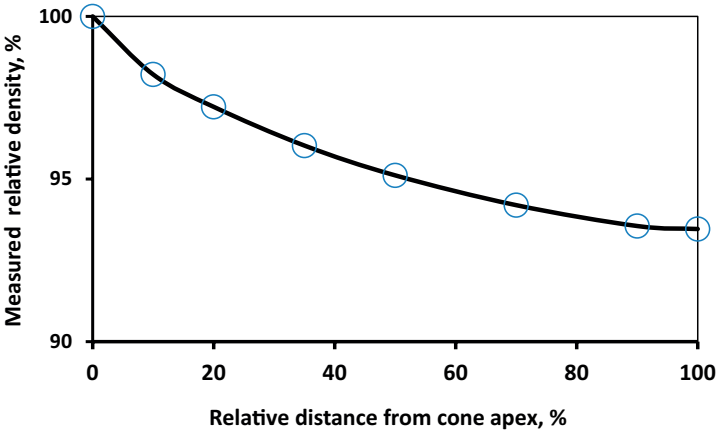

Figure 5. Real measured density of liner elements at different distances from the liner apex

The jetting analysis summary is shown in Table 5 for both studied liners; the baseline copper and the pressed copper-tungsten compacted powder. The higher liner mass of the pressed powder liner exhibited a lower mass and so lower jet tip velocity. On the other hand the lower density shown for the copper material liner showed higher jet tip velocity, but its net kinetic energy was lower than that of the copper tungsten powder liner. Therefore, the jet penetration capability of the powder jet into the tested RHA is expected to be more effcient than that of the traditional baseline copper. A detailed jetting curve of jet velocity with cumulative jet mass for both jets is shown in Figure 6, which shows both different fingerprint curves with lower jet tip velocity of the powder liner but with lower mass of its jet.

Table 5. The jetting calculation outputs for the baseline copper and the selected pressed copper-tungsten compacted powder (of the real measured density) liners

Parameter	Copper	Powder W35-Cu55
Liner mass [g]	27.25	31.10
Jet mass [g]	4.78	5.2
Jet percentage [%]	17.5	16.7
Jet kinetic energy [kJ]	43.4	44.9
Maximum jet tip velocity [m/s]	6617	6519
Maximum flow velocity [m/s]	3080	2902

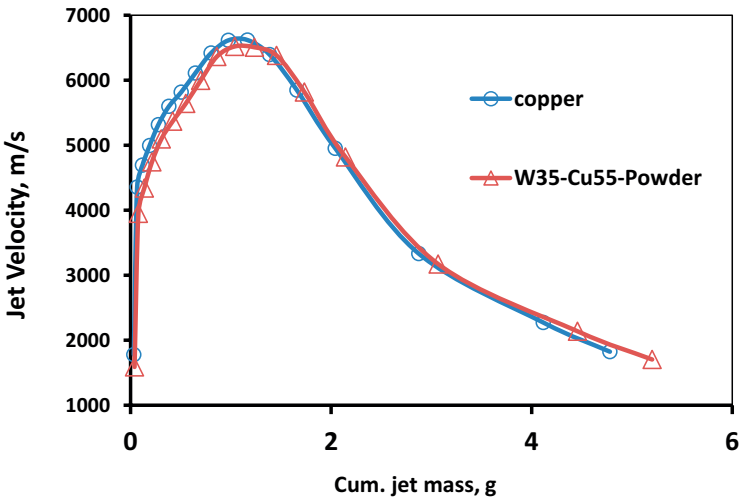

Figure 6. Sample of the jetting summaries for both liners; the Cu-W powder liner and the baseline copper one

A different profile of the liner element and its collapse to form the jet and the slug is shown in Figure 7 for both liners at 0 μs, 10 μs and 20 μs from the moment of explosive initiation. The different colours in the powder liner is shown because all the liner elements with different densities are entered into the Autodyn as a new different material with its specific real measured density based on the gas pycnometer measurements. The phase of jet formation for both jet histories is somewhat different because of two reasons; first is the jet percentage difference between the two liners, which shows higher slug mass in case of powder liner. The second reason is there is nosychronization between the two jets due to the difference in their jet velocities, which makes the copper jet faster and has its final shape at earlier stages than that of the powder one.

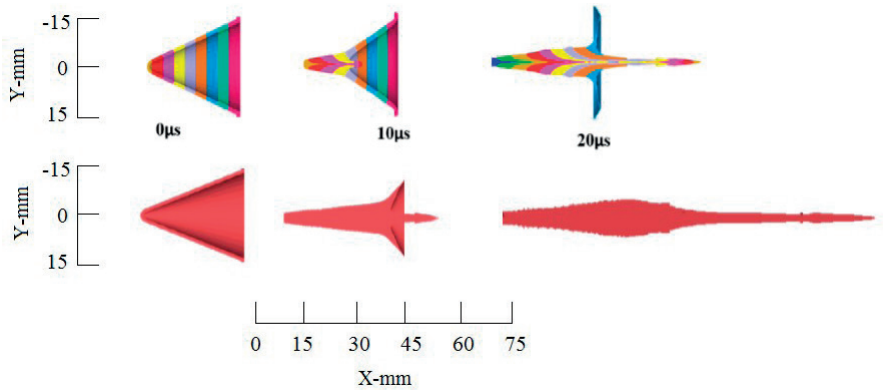

Figure 7. The jet profile at different time for copper-tungsten powder liner (top) and solid copper liner (bottom)

Figure 8 shows the calculated numerical crater profiles for the two stuided jets. The difference in their penetration depth is attributed to the diffrence in their kinetic energy, while the big entry hole in case of the copper-tungsten powder liner is accounted for its massive slug exceeding 22 g of its mass.

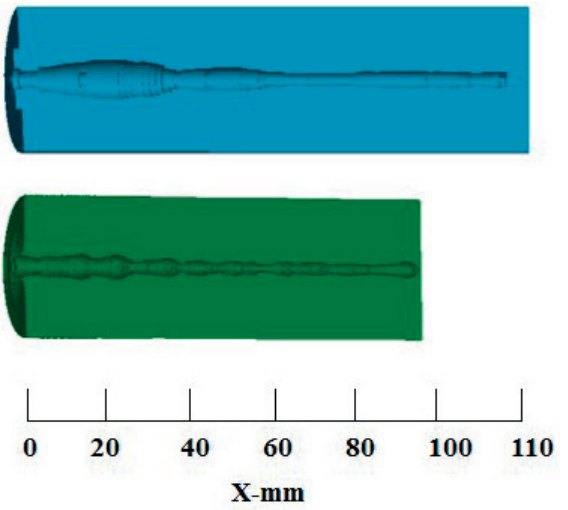

Figure 8. The crater profiles for copper-tungsten powder liner jet (top) and solid copper liner (bottom)

The effectiveness of the clean entry hole achieved with powder liner

is shown in Figures 9-10 in comparison with other massive copper slug embaded inside its hole. To show the copper slug size, the first top plate was removed from the entire welded laminated steel layers keeping the intact real final shape of the copper slug. The figure shows that the massive slug has clogged the created hole that has been created primary for target opening to allow the blast wave passes through and thus has a severe damage, which was previously described as behind armor effect.

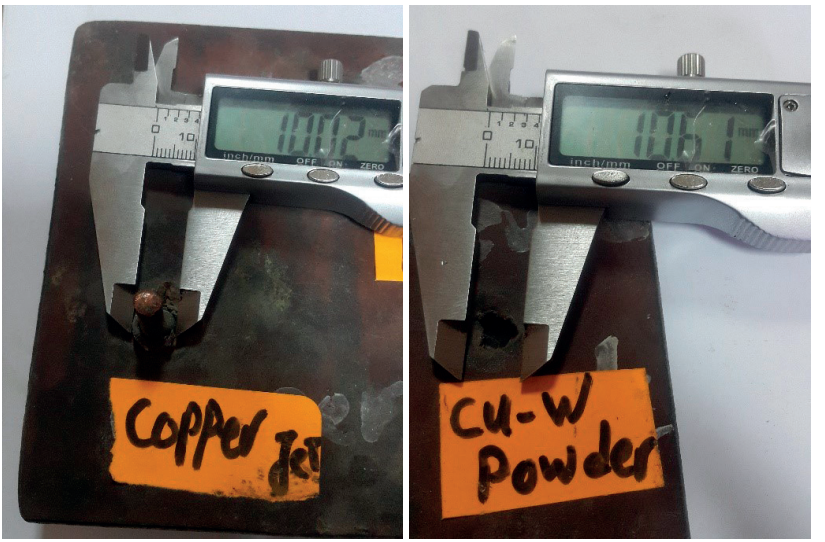

Figure 9. The front profile of the two shaped charge jets penetration into RHA steel targets for both copper-tungsten powder liner (right) and copper liner jet (left)

Figure 10. The first top perforated RHA plate for both copper liner (left) and powder non clogged hole (right)

The resulted measured penetration depths were 11.5 cm for uniaxial pressing liner and 9.3 cm for traditional baseline copper, as shown in Figures 9-10, using the same strength targets to avoide target strength effect on the penetration reduction [40]. Excess penetration of uniaxial pressing liner (24% excess) have been expected according to calculated and experimental measurment of the liners, with another advantage of the powder liner, which exhibits no massive slug that clogs the armor after it has been penetrated as that caused by traditional copper liners.

5 Conclusions

Uniaxial pressing technique, which produces non-uniform density distribution has been implemented to produce shaped charge liner used as anti-armour device capable of achieving large penetration depth without massive slug that clog the armour after penetration. Analysis of studied copper-tungsten compacted powders has shown that the liner mixture containing 35% tungsten and 55% copper by weight can achieves the fast coherent jet compared with copper liner. This mixture has been tested experimentally against RHA target in comparison with deep drawn copper as a shaped charge liners. Results demonstrated that the proposed optimized powder liner achieved enhanced larger penetration depth in comparison with baseline copper liner (*i.e.* 24% increase in the depth of penetration). As a result of the low cost of the compacted copper-tungsten powder liner and the clean penetration hole produced by its penetration, it might be candidate to replace the traditional deep drawn baseline copper for the specified anti-armour device.

References

[1] Zygmunt, B.; Wilk, Z. Formation of Jets by Shaped Charges with Metal Powder Liners. *Propellants, Explos. Pyrotech.* **2008**, *33*(6): 482-487.

[2] Bourne, B.; Cowan, K. G.; Curtis, J. P. Shaped Charge Warheads Containing Low Melt Energy Metal Liners. *Int. Symp. Ballist. Proc. 19th,* Interlaken, Switzerland, **2001**.

[3] Elshenawy, T.; Li, Q. M. Breakup Time of Zirconium Shaped Charge Jet. *Propellants, Explos. Pyrotech.* **2013**, *38*(5): 703–708.

[4] Elshenawy, T. Determination of the Velocity Difference between Jet Fragments for a Range of Copper Liners with Different Small Grain Sizes. *Propellants, Explos. Pyrotech.* **2016**, *41*(1): 69-75.

[5] Baker, E. L.; DeFisher, S.; Daniels, A.; Vuong, T.; Pham, J. Glass as a Shaped Charge Liner Material Glass as a Shaped Charge Liner Material. *Int. Symp. Ballist. Proc. 26th*, Lancaster, PA. **2011**.
[6] Reese, J. W.; Hetz, A. *Coated Metal Particles to Enhance Oil Field Shaped Charge Performance.* Patent US 7011027, **2006**.
[7] Stinson, J. S.; Nelson, S. R.; Wittman, C. L. *Method for Producing High Density Refractory Metal Warhead Liners from Single Phase Materials.* Patent US 5523048, **1996**.
[8] Walters, W.; Peregino, P.; Summers, R.; Leidel, D. A Study of Jets from Unsintered-powder Metal Lined Nonprecision Small-caliber Shaped Charges. Report no. ARL-TR-2391. Army Research Lab Aberdeen Proving Ground MD Weapons and Materials Research Directorate, USA, **2001**.
[9] Leidel, D. J.; Lawson, J. P. High Performance Powdered Metal Mixtures for Shaped Charge Liners. Patent US 7547345, **2009**.
[10] Hirsch, E.; Mayseless M. Penetration of Porous Jets. *J. Appl. Mech.* **2010**, *77(*5): 51803.
[11] Zhang, X.; Wu, C.; Huang F. Penetration of Shaped Charge Jets with Tungsten-copper and Copper Liners at the Same Explosive-to-liner Mass Ratio into Water. *Shock Waves* **2010**, *20*(3): 263-267.
[12] Glenn, L. A. *Pressure Enhanced Ppenetration with Shaped Charge Perforators.* Patent US 6223656, **2001.**
[13] Held, M. Behind Armour Effects at Shaped Charge Attacks. *Int. Symp. Ballist. Proc. 24th,* New Orleans, LA, USA, **2008.**
[14] Schwartz, A. J.; Kumar, M.; Lassila, D. H. Analysis of Intergranular Impurity Concentration and the Effects on the Ductility of Copper-shaped Charge Jets. *Metall. Mater. Trans. A* **2004**, *35*(9): 2567-2573.
[15] Held, M. Liners for Shaped Charges. *J. Battlefield Tech.* **2001**, *4*:1-7.
[16] Elbeih, A.; Wafy, T. Z.; Elshenawy, T. Performance and Detonation Characteristics of Polyurethane Matrix Bonded Attractive Nitramines, *Cent. Eur. J. Energ. Mater.* **2017***, 14*(1)*:* 77-89.
[17] Sućeska, M. *Test Methods for Explosives.* Springer, Heidelberg, **1995**; ISBN 978-1-4612-0797-9.
[18] Šelešovský, J.; Pachmáň, J. Probit Analysis − a Promising Tool for Evaluation of Explosive's Sensitivity. *Cent. Eur. J. Energ. Mater.* **2010**, *7*(4): 269-278.
[19] Zeman, S.; Yan, Q.-L.;Elbeih, A. Recent Advances in the Study of the Initiation of Energetic Materials Using the Characteristics of their Thermal Decomposition. Part II. Using Simple Differential Thermal Analysis. *Cent. Eur. J. Energ. Mater.* **2014**, *11*(3): 395-404.
[20] Pelikan, V.; Zeman, S.; Yan,Q.-L.;Erben, M.; Elbeih, A.; Akštein, Z. Concerning the Shock Sensitivity of Cyclic Nitramines Incorporated into a Polyisobutylene Matrix. *Cent. Eur. J. Energ. Mater.* **2014**, *11*(2): 219-235.
[21] Elbeih, A.; Mohamed, M.; Wafy, T. Sensitivity and Detonation Characteristics of Selected Nitramines Bonded by Sylgard Binder. *Propellants Explos. Pyrotech.*

2016, *41(*6): 1044-1049.
[22] Sućeska, M. Calculation of Detonation Parameters by EXPLO5 Computer Program. In: *Explosion, Shock Wave and Hypervelocity Phenomena in Materials.* ISBN 978-087849-950-2. Periodical: *Mater. Sci. Forum* **2004**, *465*: 325.
[23] Pugh, E. M.; Eichelberger, R. J.; Rostoker, N. Theory of Jet Formation by Charges with Lined Conical Cavities. *J. Appl. Phys.* **1952**, *23*(5): 532-536.
[24] Elshenawy, T.; Li, Q. Influences of Target Strength and Confinement on the Penetration Depth of an Oil Well Perforator. *Int. J. Impact Eng.* **2013**, *54*: 130-137.
[25] Tarver, C. M.; Tao, W. C.; Lee, C. G. Sideways Plate Push Test for Detonating Solid Explosives. *Propellants Explos. Pyrotech.* **1996**, *21(*5): 238-246.
[26] Lan, I.; Hung, S.C.; Chen, C.Y.; Niu, Y.M.; Shiuan, J.H. An Improved Simple Method of Deducing JWL Parameters from Cylinder Expansion Test. *Propellants Explos. Pyrotech.* **1993**, *18(*1): 18-24.
[27] Elek, P. M.; Džingalašević, V. V.; Jaramaz, S. S; Micković, D. M. Determination of Detonation Products Equation of State from Cylinder Test: Analytical model and numerical analysis. *Thermal Science* **2015**, *19*(1): 35-48.
[28] Kato, H.; Kaga, N.; Takizuka, M.; Hamashima, H.; Itoh, S. Research on the JWL Parameters of Several Kinds of Explosives. *Mater. Sci. Forum* **2004**, *465-466*: 271.
[29] *AUTODYN® Jetting Tutorial.* 3rd Revision, Century Dynamics, USA, **1997.**
[30] Valat-Villain, P.; Durinck, J.; Renault, P. O. Grain Size Dependence of Elastic Moduli in Nanocrystalline Tungsten. *Journal of Nanomaterials* **2017**, DOI: 10.1155/2017/3620910.
[31] Cowan, G. R.; Holtzman, A. H. Flow Configurations in Colliding Plates: Explosive Bonding. *Journal of Applied Physics* **1963**, *34*(4): 928-939.
[32] Chou, P. C.; Carleone, J.; Karpp, R. R. Criteria for Jet Formation from Impinging Shells and Plates. *J. Appl. Phys.* **1976**, *47*(7): 2975-2981.
[33] Harrison, J. T. Improved Analytical Shaped Charge Code: basc. Report no. ARBRL-TR-02300. US Army Ballistic Research Laboratory, Aberdeen Proving Ground, Maryland, USA, **1981.**
[34] Walker, J. D. Incoherence of Shaped Charge Jets. *AIP Conference Proceedings* **1994**, *309*(1): 1869-1872.
[35] Walters, P.; Zukas, J. *Fundamentals of Shaped Charge.* Wiley Interscience Publication, New York, USA **1989**; ISBN 9780471621720.
[36] Shekhar, H. Theoretical Modelling of Shaped Charges in the Last Two Decades (1990-2010): A Review. *Cent. Eur. J. Energ. Mater.* **2012**, *9*(2): 155-185.
[37] Maritz, M. F.; Werneyer, K. D.; Mostert, F. J. An Analytical Penetration Model for Jets with Varying Mass Density Profiles. *Int. Symp. Ballist. Proc. 22nd,* Vancouver, Canada, **2005**.
[38] Grove, B.; Walton, I. Shaped Charge Jet Velocity and Density Profiles. *Int. Symp. Ballist. Proc. 23rd,* Tarragona, Spain, **2007**.
[39] Elshenawy, T.; Elbeih, A.; Li, Q. M. A Modified Penetration Model for Copper-Tungsten Shaped Charge Jets with Non-uniform Density Distribution. *Cent. Eur.*

J. Energ. Mater. **2016**, *13*(4): 927-943.
[40] Elshenawy, T.; Elbeih, A.; Li, Q. M. Influence of Target Strength on the Penetration Depth of Shaped Charge Jets into RHA Targets. *Int. J. Mech. Sci.* **2018**, *136*: 234-242.

Received: April 9, 2018
Revised: December 5, 2018
First published online: December 17, 2018